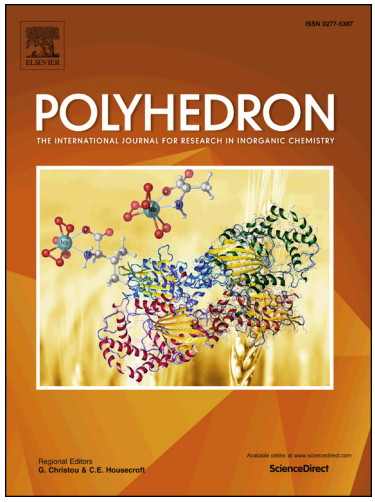

Phosphatase activity and DNA binding studies of dinuclear phenoxo-bridged zinc(II) complexes with an N,N,O-donor ligand and halide ions in a rare *cis*-configuration

Monika Sheoran, Kishalay Bhar, Tanveer A. Khan, Anuj K. Sharma, Sunil G. Naik

PII: S0277-5387(17)30233-4
DOI: http://dx.doi.org/10.1016/j.poly.2017.03.037
Reference: POLY 12552

To appear in: *Polyhedron*

Received Date: 22 December 2016
Revised Date: 17 March 2017
Accepted Date: 19 March 2017

Please cite this article as: M. Sheoran, K. Bhar, T.A. Khan, A.K. Sharma, S.G. Naik, Phosphatase activity and DNA binding studies of dinuclear phenoxo-bridged zinc(II) complexes with an N,N,O-donor ligand and halide ions in a rare *cis*-configuration, *Polyhedron* (2017), doi: http://dx.doi.org/10.1016/j.poly.2017.03.037

Phosphatase activity and DNA binding studies of dinuclear phenoxo-bridged zinc(II) complexes with an N,N,O-donor ligand and halide ions in a rare *cis*-configuration

Monika Sheoran[a], Kishalay Bhar[a], Tanveer A. Khan[a], Anuj K. Sharma[a] and Sunil G. Naik[a]*

[a]*Department of Chemistry, School of Chemical Sciences and Pharmacy, Central University of Rajasthan, NH-8, Bandarsindri, Ajmer Distt. Rajasthan, INDIA 305817*

Abstract

Three new dinuclear zinc(II) complexes of the types $[Zn_2(L)_2(Cl)_2].2(CH_3OH)$ (**1**) and $[Zn_2(L)_2(X)_2]$ (HL = 2-((2-(dimethylamino)ethyl)amino)methyl)phenol; X = Br for **2** and I for **3**), having a rare *cis*-configuration of the halide ions, were isolated using the one-pot synthesis of the building components in appropriate molar ratios and characterized. X-ray structural studies reveal that **1-3** contain a discrete dinuclear unit bridged by two phenoxo oxygen atoms of the deprotonated Schiff base ligand (HL) and adopt an overall rare *cis*-configuration where two halide ions are on the same side of the Zn-Zn axis and the ligand occupies the other side. Each Zn(II) centre in **1-3** has a distorted square pyramidal geometry with a ZnO_2N_2X chromophore (X = Cl for **1**; Br for **2**; I for **3**). The initial rate values for the hydrolysis of 4-nitrophenylphosphate to 4-nitrophenolate by the complexes **1**-**3** are respectively 590, 334 and 705 min^{-1}. The complexes show an external binding propensity to calf thymus DNA with binding constant values 9.45 x 10^2, 7.06 x 10^2 and 6.51 x 10^2 M^{-1} for **1**, **2** and **3** respectively.

- *Keywords:* Dinuclear zinc(II) halides; Phenoxo bridge; Schiff base; Phosphatase activity; DNA binding

---

*Corresponding author.
sunilnaik@curaj.ac.in

1. Introduction

Metal-ion catalyzed reactions have gained a lot of importance in the past few years, with zinc containing metalloenzymes constituting by far the widest category [1,2]. The Zn(II) active site is present in a number of fundamental enzyme classes, like transferases, hydrolases, oxidoreductases, lyases, isomerases and ligases [3-9]. The hydrolysis of phosphate esters is of particular interest because it is involved in biosynthesis energy transduction, regulation of protein function and control of secondary messengers [10,11]. Among the versatile range of enzymatic behaviour of the zinc(II) ion [12-15], phosphatase activity is an important function of various functional mimics of phosphoesterases. Various dinuclear Zn(II) complexes [16-22] have been studied over time as phosphate ester models, taking into account their extraordinary Lewis acidity, nucleophile generation, redox rigidity, leaving group stabilization and physiological relevancy [23-25]. In order to develop new anti-cancer drugs, the binding mechanism of the complex with DNA [26-28] should be studied. The intercalative mode is the most important mode in which transition metal complexes can intercalate between the pair-bases of double helix DNA, forming π-π overlapping interactions. It is the interaction that changes the DNA conventional behaviour and so the transition metal complexes possess a very broad application in the field of bio-inorganic chemistry. Of late, Schiff base bridged dinuclear Zn(II) complexes have gained lot of significance owing to their good DNA interaction behaviour [18,29-32]. To explore the chemistry of such phosphatase activity and DNA interaction, herein we have synthesised and characterised three new dinuclear zinc(II) halide complexes containing a tridentate Schiff base, 2-((2-(dimethylamino)ethyl)amino)methyl)phenol (HL, Scheme 1).

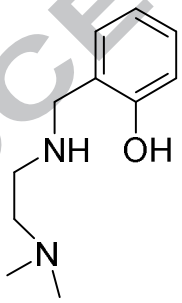

HL

Scheme 1. The tridentate Schiff base, 2-((2-(dimethylamino)ethyl)amino)methyl)phenol (HL).

2. Experimental

2.1. Materials

All the chemicals used in the present study were obtained from different commercial sources. Solvents were distilled before use according to standard procedures. The anhydrous zinc halide salts ($ZnCl_2$, $ZnBr_2$) were obtained from CDH, India. ZnI_2 was synthesized by a standard procedure using Zn metal and iodine. Water used in the physical measurements was Milli-Q grade. The (p-nitrophenyl) phosphate (PNPP) used for the catalytic studies was purchased from Spectrochem, India and re-crystallized from ethanol/water.

2.2. Physical measurements

Elemental analyses were performed on a Perkin–Elmer 2400 CHNS elemental analyzer. Infrared spectra were recorded at room temperature using a Perkin Elmer FTIR spectrometer in the 4000-400 cm^{-1} range. The ^1H NMR spectra were recorded in $CDCl_3$ and DMSO-d_6 solvent on a Bruker-500 MHz spectrometer at 25°C. UV-Vis spectra and kinetic studies were performed at room temperature on an Agilent Technologies Cary 100 UV-Vis spectrophotometer equipped with multiple cell-holders. Fluorescence measurements were done on a Perkin Elmer LS55 fluorescence spectrophotometer at 25°C.

2.3. X-ray crystallography

Crystallographic data of compounds **1**-**3** were collected on a Bruker APEX-II CCD diffractometer at 296 K (for **1**) and 100 K (for **2** and **3**) using graphite monochromated Mo Kα radiation (λ = 0.71073 Å). For unit cell determination, the single crystal was exposed to X-rays for 10 s in three sets of frames. The detector frames were integrated by use of the program SAINT [33] and multi-scan absorption corrections were performed using the SADABS program [34]. The structures were solved by direct methods and refined by full-matrix least-squares methods based on F^2 using SHELXS-97 [35] and SHELXL-97 [35]. All the non-hydrogen atoms were refined with anisotropic displacement parameters, whereas hydrogen atoms were placed in calculated positions when possible and given isotropic *U* values 1.2 times that of the atom to which they are bonded. The NH hydrogen atoms of the ligands in complex **2** were not located. The crystal of compound **1** is a twin with twin law 010 100 00-1 and BASF 0.01174. In the final difference Fourier maps, the residual maximum and minimum were 0.221 and -0.287 e $Å^{-3}$ for **1**, 1.627 and -1.730 e $Å^{-3}$ for **2** and 1.676 and -1.219 e $Å^{-3}$ for **3**. Materials for publication were prepared using SHELXTL [35], PLATON

[36] and Mercury [37] programs. A summary of the crystallographic data and structure determination parameters are given in Table 1.

2.4. Synthesis

2.4.1. 2-((2-(dimethylamino)ethyl)amino)methyl)phenol(HL)

The Schiff base (HL) was synthesized using a reported procedure [38]. A solution of salicylaldehyde (1 g, 8.18 mmol) in methanol was refluxed with *N,N*-dimethylethylenediamine (0.72 g, 8.18 mmol) for 3 h. The reaction mixture was cooled to room temperature and then $NaBH_4$ (0.9 g, 23.7 mmol) was added at 0°C. The reaction mixture was stirred for a further 30 minutes and HCl was added to adjust the pH to 1 or 2 initially, and followed by addition of NaOH to attain pH 12. The resulting mixture was extracted with $CHCl_3$ and dried over anhydrous sodium sulfate. On evaporating the solvent, a yellow solid was obtained (Yield: 1.51 g, 95%). Elemental analysis calcd. for $C_{11}H_{18}N_2O$: C, 68.01; H, 9.34; N, 14.42; found: C, 68.15; H, 9.40; N, 14.55% .^{1}H NMR (500MHz, $CDCl_3$, 298K) δ, ppm: 6.7-7.5 (4H, aromatic), 3.9 (2H, s, CH_2), 2.7 (2H, t, CH_2), 2.4 (2H, t, CH_2), 2.23 (6H, s, CH_3).^{13}C NMR (500 MHz, $CDCl_3$, 298K) δ, ppm: 158.35, 128.60, 128.32, 122.0, 118.87, 116.33, 58.71, 52.41, 45.71, 45.40. ^{13}C (DEPT) NMR (500 MHz, $CDCl_3$, 298K) δ, ppm: 128.60, 128.32, 122.0, 118.87, 116.33, 58.71, 52.41, 45.71, 45.40. FTIR (KBr, cm^{-1}): ν(N-H) 3010, ν(C-N) 1606. UV-vis, λ_{max} (nm) (ε_{max}, $dm^3\ mol^{-1}\ cm^{-1}$): 277 (2.8×10^3).

*2.4.2. $[Zn_2(L)_2(Cl)_2].2(CH_3OH)$ (**1**)*

A solution of HL (1 g, 5.15 mmol.) in methanol (20 mL) was stirred with NEt_3 (0.52 g, 5.15 mmol) at room temperature for 15 minutes. A methanolic solution (10 mL) of $ZnCl_2$ (0.70 g, 5.15 mmol) was added to the above solution, with stirring. The resulting white solid that formed was filtered and dried (Yield: 1.30 g, 86%). Elemental analysis calcd. for $C_{24}H_{42}Cl_2N_4O_4Zn_2$: C, 44.19; H, 6.49; N, 8.59; found: C, 44.10; H, 6.52; N, 8.63%. ^{1}H NMR (500MHz, DMSO-d_6, 298K) δ, ppm: 6.5-7.3 (8H, aromatic), 2.38-3.86 (12H, aliphatic), 2.19 (12H, CH_3). FTIR (KBr, cm^{-1}): ν(N-H) 3008, ν(C-N) 1600. UV-vis, λ_{max} (nm) (ε_{max}, $dm^3\ mol^{-1}\ cm^{-1}$): 283 (6.1×10^4), 371 (7.01×10^2).

*2.4.3.$[Zn_2(L)_2(Br)_2]$ (**2**)*

Complex **2** was prepared by stirring a solution of HL (0.59 g, 3.06 mmol) and $ZnBr_2$ (0.69 g, 3.06 mmol) in methanol for 30 minutes. The resulting white solid was filtered and dried (Yield: 0.87 g, 84%). Elemental analysis calcd. for $C_{22}H_{34}Br_2N_4O_2Zn_2$: C, 39.02; H, 5.06; N, 8.27; found: C, 39.11; H, 5.08; N, 8.32%. ^{1}H NMR (500MHz, DMSO-d_6, 298K) δ,

ppm: 6.5-7.3 (8H, aromatic), 2.20 (12H, CH_3), 2.38-3.95 (12H, aliphatic). FTIR (KBr, cm^{-1}): ν(N-H), 3002, ν(C-N), 1600.UV-vis, λ_{max} (nm) (ε_{max}, $dm^3\,mol^{-1}\,cm^{-1}$): 282 (6.2×10^4).

*2.4.4.[$Zn_2(L)_2(I)_2$] (**3**)*

Complex **3** was prepared by the same procedure as that of **2** by using anhydrous ZnI_2 (0.90 g, 2.85 mmol) as the metal salt. A white coloured solid was filtered and dried (Yield: 0.9 g, 90%). Elemental analysis calcd. for $C_{22}H_{34}I_2N_4O_2Zn_2$: C, 34.26; H, 4.44; N, 7.27; found: C, 34.20; H, 4.52; N, 7.32%. ^{1}H NMR (500MHz, DMSO-d_6, 298K) δ, ppm: 6.3-7.1 (8H, aromatic), 2.26 (12H, CH_3), 2.49-4.13 (12H, aliphatic). FTIR (KBr,cm^{-1}): ν(N-H) 3002, ν(C-N) 1600.UV-vis, λ_{max} (nm) (ε_{max}, $dm^3\,mol^{-1}\,cm^{-1}$): 284 (6.5×10^4).

2.5. Hydrolysis of phosphate ester

Disodium (4-nitrophenyl)phosphatehexahydrate (4-NPP) was used as the substrate to study the Phosphatase activity. All experiments were done in a 97.5% DMF/H_2O mixture [17,39,40]. Solutions of the zinc complexes and substrate 4-NPP were freshly prepared and the total volume maintained was 3 mL. The kinetic data was collected after 2 h of the reaction when 2% of the reaction was complete. The rate of hydrolysis of 4-NPP in the presence of zinc complexes **1-3** was measured by an initial rate method, following the increase in absorption at 423 nm due to the formation of the 4-nitrophenolate ion (ε, 18500 $M^{-1}cm^{-1}$) at 25 °C [39]. The kinetic experiments were performed both at variable substrate or complex concentration, keeping either the complex or the substrate concentration constant. The study was comprised of 5 sets of experiments having the complex concentration as 0.05 mmol and the substrate concentration as 0.5 (10 equiv.), 0.7 (14 equiv.), 1.0 (20 equiv), 1.2 (24 equiv.) and 1.5 (30 equiv.) mmol. The stock solutions of 2.5 mM of the complexes and substrate were prepared in a DMF:H_2O mixture. The reactions were performed by injecting 60 µL of the complex and different volumes of the substrate (0.6, 0.84, 1.2, 1.44 and 1.8 mL) in a cuvette and making the final volume to 3 mL with solvent. The visible absorption increase was recorded for a total period of 2 h, at intervals of 5 min. All the recordings were performed at least twice and average values were taken for the data. The reactions were corrected for the degree of ionization of 4-nitrophenolate at 25 °C using the molar extinction coefficient for 4-nitrophenolate at 423 nm [40]. The final absorbance values for each set were obtained after 72 h.

2.6. Control experiments

Control experiments were performed for the zinc salts and the ligand to identify any individual effects on the hydrolysis of 4-NPP. There was no noticeable change in the results.

2.7. Fluorescence spectroscopy method

The intrinsic fluorescence measurements of DNA with the zinc complexes **1-3** were done on a Perkin Elmer LS55 Fluorescence spectrophotometer at room temperature. The concentrations of DNA and ethidium bromide (EB) were kept constant at 37 μM and 10.5 μM, respectively in all the experiments and the complex concentration was varied from 0 to 430 μM. The excitation and emission slit widths were fixed at 15 and 20 nm, respectively. The emission spectra were recorded in the wavelength range λ_{em}= 490-800 nm by exciting the DNA at the wavelength λ_{ex} = 480 nm. Stock solutions (2 mM) of thte zinc complexes were prepared in a 95% H_2O/DMSO mixture using Tris-10mM/EDTA 1 mM ($T_{10}E_1$) buffer.

3. Results and discussion

3.1. Syntheses and spectroscopic studies

Complexes **1-3** were isolated as white solids by mixing a 1:1 molar ratio of the zinc(II) halides and the Schiff base (HL) in the presence of triethyl amine in MeOH at room temperature. All the reactions were reproducible, as was evident from repetitive spectral behaviours. Details of sequential reactions are summarized in Scheme 2.

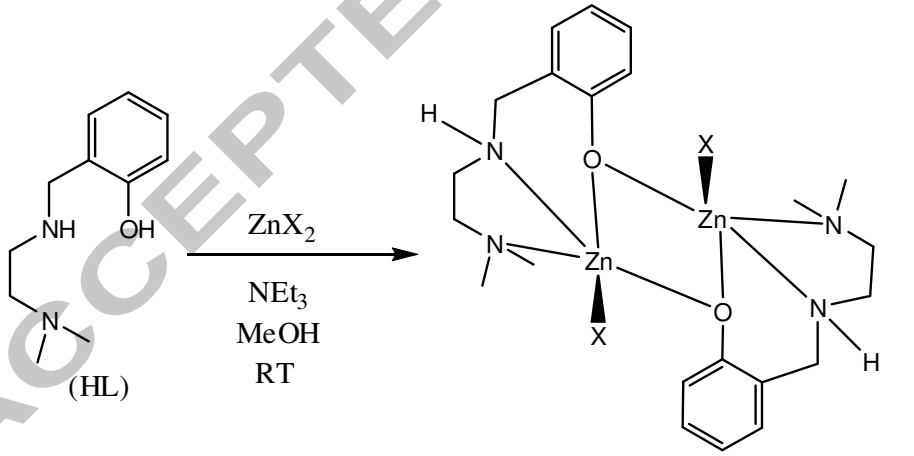

Complexes (X = Cl, **1**; Br, **2** and I, **3**)

Scheme 2. Synthesis of the zinc(II) complexes **1-3**.

The compounds were characterized using FTIR, UV-Vis and NMR spectroscopy. The spectroscopic results are in good agreement with the formulations **1**-**3**. All the

compounds are stable over a long period of time in powdery or crystalline form. **1-3** are soluble in a wide range of common non-aqueous solvents, such as acetonitrile, dimethylformamide and dimethylsulfoxide. The ^{1}H NMR spectrum of HL in $CDCl_3$ shows four signals in the aliphatic region, consisting of two singlets and two triplets. In the aromatic region (δ 6.7-7.5 ppm), four signals are observed (Supporting Information, Fig. S1) for HL. The ligand was further characterized by ^{13}C NMR and ^{13}C (DEPT) NMR spectra in $CDCl_3$, which showed the presence of aromatic carbon signals at δ 158.35-116.33 ppm in addition to CH_2- and $-CH_3$ signals at δ 58.1-45.40 ppm (Supporting Information, Figs. S2 and S3). The ^{1}H NMR spectra of the metal complexes **1-3** taken in DMSO-d_6 have a similar type of spectrum as HL, with slightly shifted values (Supporting Information, Figs. S4-S6). On comparing the spectra of the ligand and diamagnetic zinc(II) complexes, it was found that there is not much difference because the coordinated and uncoordinated groups have same kind of magnetic environment. Thus, from these NMR results it appears that the solution state structural formulations are in good agreement with their crystalline form. In DMF solution, the ligand (HL) exhibits an intraligand charge transfer band at 277 nm. The corresponding complexes **1**-**3** in DMF show a strong ligand-based [39,41] transition at ca. 280 nm (Supporting Information, Fig. S7). In addition, complex **1** displays a low energy ligand to metal charge transfer band [17] at 371 nm, which is probably due to a $PhO^{-}\rightarrow Zn^{II}$ transition or to a mixture of the former and a $Cl^{-}\rightarrow Zn^{II}$ transition. In the FTIR spectra, the free Schiff base (HL) and complexes **1**-**3** show weak to medium stretches in the 3000-3010 cm^{-1} region, corresponding to ν(N-H), and a strong band at ca. 1600 cm^{-1} which is attributed to ν(C-N) stretching [42] (Supporting Information, Fig. S8- S11).

3.2. Crystal structures

Single crystal X-ray diffraction studies revealed that compounds $[Zn_2(L)_2(Cl)_2].2(CH_3OH)$ (**1**), $[Zn_2(L)_2(Br)_2]$ (**2**) and $[Zn_2(L)_2(I)_2]$ (**3**) contain discrete dinuclear units formed by two Zn(II) ions [Zn(1) and Zn(1a) (a = -x,1-y,z) for **1** and Zn(1) and Zn(2) for **2** and **3**], bridged by the two phenoxo oxygen atoms [O(1) and O(1a) for **1** and O(1) and O(2) for **2** and **3**] of the deprotonated Schiff base ligands (L). Complex **1** has an inversion center and crystallises in the *orthorhombic* system with the space group *Aba2*, whereas complexes **2** and **3** are located on general positions and crystallise in the *triclinic* system with the space group *P-1*. Each Zn(II) center is penta-coordinated by two $\mu_{O,O}$-

bridging phenoxo O-atoms, two N atoms of the amine groups of the deprotonated Schiff base ligand and one terminal halide anion (Figs. 1-3). The ZnO_2N_2X chromophores (X = Cl for **1**; X = Br for **2** and I for **3**) may be described as distorted square pyramids (SP), and their Addison parameter [43] τ is 0.14 for Zn1 and Zn1a in **1**, 0.038 for Zn1 and 0.12 for Zn2 in **2** and 0.086 for Zn1 and 0.064 for Zn2 in **3**. The two amine N atoms (N1, N2 for Zn1 and N1a, N2a for Zn1a in **1** and N1, N2 for Zn1 and N3, N4 for Zn2 in **2** and **3**) along with two $\mu_{O,O}$-bridging phenoxo O atoms (O1 and O1a in **1**; O1 and O2 in **2** and **3**) form an equatorial plane, whereas the terminal halide anions (Cl1 for Zn1 and Cl1a for Zn1a in **1**, Br2 for Zn1 and Br4 for Zn2 in **2**, I1 for Zn1 and I2 for Zn2 in **3**) occupy the axial positions. It is interesting to note that **1**-**3** adopt an overall rare *cis*-configuration (Figs. 1-3), where two halide ions (Cl1 and Cl1a in **1**, Br2 and Br4 in **2,** I1 and I2 in **3**) are on the same side of the Zn-Zn axis and the ligand (HL) occupies the other side. To the best of our knowledge only four such dinuclear complexes [30,45] have been reported so far. The Zn_2O_2 bridging core in the dinuclear units of **1-3** is asymmetric in nature, with two different Zn-O distances (Table 2) which is consistent with similar diphenolato-bridged dinuclear zinc complexes [17,30,44-47]. The differences in the two Zn-O distances is found to be 0.020 Å in **1**, 0.095, 0.074 Å in **2** and 0.107, 0.068 Å in **3,** indicating that the Zn_2O_2 moiety in **2** and **3** is less symmetrical, whilst in **1** it is symmetrical. The *cis*-oriented Zn-X distances, along with Zn-N(amine) lengths (Table 2), are consistent with the literature data [17,30,44-47]. In dinuclear **1-3**, the two zinc(II) centers are 3.217, 3.220 and 3.209 Å apart from each other, respectively.

It is well known that weak non-covalent bonds, such as C-H...X (X = O, N, S, halogens), C-H...π, anion...π interactions and π... π-stacking, though weaker than classical hydrogen bonds, play an important role in the conformation, crystal packing, supramolecular assembly and physicochemical properties. Such non-covalent interactions are at the core of most chemical and biological processes and hence knowledge of their nature, strength, occurrence and consequences is of paramount importance. Weak inter-molecular C-H...Cl, O-H...Cl, C-H...O and N-H...O interactions (Table 3) in **1** propagate along the *(100)*-plane, giving rise to a 2D zigzag sheet-like crystalline architecture (Fig. 4). On the other hand, weak C-H...Br (in **2**) and N-H...I, C-H...I (in **3**) interactions combine individual dinuclear units along the *a-axis*, forming 1D chains (Table 3, Fig. 5).

3.3. Phosphatase activity and kinetic study

The phosphatase activity of complexes **1-3** was studied using the disodium salt of (4-nitrophenyl) phosphate hexahydrate. The hydrolytic tendency of **1-3** was determined spectrophotometrically by monitoring the evolution of 4-nitrophenolate (λ_{max} = 423 nm) through a wavelength scan from 200 to 800 nm in aqueous DMF [40]. The change in spectral behaviour of **1** is shown in Fig.6, as a representative case, and those of the other complexes (**2** and **3**) are given in the Supporting Information (Figs. S12 and S13).

The kinetic behaviour of complexes **1-3** was studied by the initial slope method, following the rate of increase in absorption of the band corresponding to the formation of 4-nitrophenolate at 423 nm. The plot of $\log[A_\infty/A_\infty - A_t]$ values versus time gave the initial rate constants, V (M min^{-1}) for the zinc complexes (Fig. 7 for **1**). The dependence of the rate constants on five different substrate concentrations gave first order kinetics at lower concentrations, but deviates from unity at higher concentrations (Fig. 8 for **1**). The kinetic parameters (V_{max}, K_M, K_{cat}) for the catalyzed reactions of the zinc complexes were determined from the Lineweaver-Burk plot of 1/V versus 1/[S], as per the Michaelis Menten approach of enzymatic kinetics. Similar plots for complexes **2** and **3** are given in the Supporting Information (Figs. S14 and S15). All the kinetic parameters are given in Table 4. Control experiments were performed to determine any role of the ligand (HL) and zinc(II) halide salts in the catalytic reaction. The results (Supporting Information, Figs. S16 and S17) indicate no appreciable change. The catalytic activity order of the complexes, **3** > **1** > **2**, shows a direct correspondence to the Zn...Zn separation (3.217 Å for **1**, 3.220 Å for **2** and 3.209 Å for **3**), indicating the shorter Zn...Zn distance is better suited to accommodate the phosphate group.

3.4. DNA binding study

To understand the binding of the zinc complexes **1-3** with DNA and the fluorescence quenching, 0-430 µM of the zinc complexes were successively added to DNA (37 µM) solutions containing 10.5 µM ethidium bromide (EB) in $T_{10}E_1$ buffer. The samples were excited at 480nm and the emission spectra were observed at 594 nm. EB strongly intercalates between the DNA base pairs and gives intense fluorescence [30]. Representative emission spectra of EB bound to DNA in the absence and presence of **1** are shown in Fig.9.

There is a steady decrease in the intensity of the emission maxima upon addition of complex **1**, leading to saturation levels. The binding constant was calculated using the Stern-Volmer equation [48].

$$I_o/I = 1 + K_{SV}[R]$$

where I_o and I are the fluorescence intensities in the absence and presence of the zinc complexes respectively, K_{SV} is the Stern-Volmer quenching constant, [R] is the concentration of the quencher (complexes). The ratio of the slope to the intercept in the plot of I_o/I vs [R] gives the value of K_{SV} (Fig.10). For complexes **2** and **3**, the results are shown in the Supporting Information (Figs. S18-S21). The Stern-Volmer constant K_{sv} for **1**, **2** and **3** are 9.45×10^2, 7.06×10^2, 6.51×10^2 respectively, indicating weak external binding to CT-DNA. These results show that **1** has a high binding constant with CT-DNA as compared with the binding constants of **2** and **3**.

4. Conclusion

Three new dinuclear zinc(II) halide complexes (**1-3**) containing a tridentate N,N,O-donor Schiff base and having a rare *cis*-configuration of the halide ions were synthesised and characterized using analytical and spectroscopic methods. Single crystal X-ray studies reveal a phenoxo bridged dinuclear nature of the complexes with the rare *cis*-configuration, where the terminal halide ligands are on the same side of the Zn-Zn axis and the Schiff bases are on the other side. The complexes show moderate catalytic activity towards the hydrolysis of the disodium salt of (4-nitrophenyl)phosphate hexahydrate and weak external binding to CT-DNA. We are now active in extending such work using other NNO-donor ligands and zinc(II) halides.

Conflict of interest

Authors declare that there are no conflicts of interests.

Acknowledgements

Financial support from the CSIR [Grant No. 01(2840/16/EMR-II)] and DST-SERB (Grant No. EMR/2015/000764), New Delhi, India, and the Central University of Rajasthan is gratefully acknowledged. MS and TAK are grateful to the UGC and KB is grateful to DST-SERB, New Delhi, India for fellowships. Instrumental facilities at the Department of Chemistry, Central University of Rajasthan are also acknowledged. AKS thanks the DST-INSPIRE program for research grant IFA-13, CH-97. We are thankful to the Department of Chemistry, IIT, Jodhpur for the X-ray crystallographic facility.

Appendix A. Supplementary materials

CCDC 1522603, 1522604 and 1522605 contain the supplementary crystallographic data for **1-3**, respectively. These data can be obtained free of charge from The Cambridge Crystallographic Data Centre via www.ccdc.cam.ac.uk/data_request/cif. Additionally, the NMR, Mass, UV-Vis and FTIR spectra of the ligand (HL) and complexes **1-3**, the graphs of phophatase activity and DNA binding studies of complexes **2** and **3** are submitted.

References

1. D.E. Wilcox, Chem. Rev. 96 (1996) 2435.
2. L.J. Daumann, G. Schenk, D.L. Ollis, L.R. Gahan, Dalton Trans. 43 (2014) 910.
3. B.L. Vallee, D.S. Auld, Acc. Chem. Res. 26 (1993) 543.
4. M. Hambidge, N. Krebs, J. Pediatr. 135 (1999) 661.
5. G.A. Eby, J. Antimicrob. Chemother. 40 (1997) 483.
6. A. Gadomski, J. Am. Med. Assoc. 279 (1998) 1999.
7. M.L. Cleveland Macknin, Clin. J. Med. 66 (1999) 27.
8. D.G. Barceloux. J. Toxicol. Clin. Toxicol. 37 (1999) 279.
9. D.R. Williams, Coord. Chem. Rev. 186 (1999) 177.
10. R.C.H. Jin SeogSeo, Daniel Williams, Jik Chin, J. Am. Chem. Soc. 120 (1998) 9943.
11. F.H. Westheimer, Science 235 (1987) 4793.
12. M.J. Jedrjezas, P. Setlow, Chem. Rev. 101 (2001) 607.
13. M. Subat, K. Woinaroschy, C. Gerstl. B. Sarkar, W. Kaim, B. Konig, Inorg. Chem. 47 (2008) 4661.
14. J. Wetson, Chem. Rev. 105 (2005) 2151.
15. M.A.R. Raycroft, C. Tony Liu, R. S. Brown. Inorg. Chem. 51 (2012) 3846.
16. P. Chakraborty, J. Adhikary, R Sanyal, A. Khan, K. Manna, S. Dey, E. Zangrando, A. Bauzá, A. Frontera, D. Das, Inorg. Chim. Acta 421 (2014) 364.
17. (a) P. Kundu, P. Chakraborty, J. Adhikary, T. Chattopadhyay, R.C. Fischer, F.A. Mautner, D. Das, Polyhedron 85 (2015) 320; (b) R. Sanyal, P. Chakraborty, E. Zangrando, D. Das, Polyhedron 97 (2015) 55.
18. S. Anbu, S. Kamalraj, B. Varghese, J. Muthumary, M. Kandaswamy, Inorg. Chem. 51 (2012) 5580 and references therein.
19. K. Abe, J. Izumi, M. Ohba, T Yokoyama, H. Okawa. Bull. Chem. Soc. Jpn. 74 (2001) 85.
20. S. Brooker, T.C. Davidson, Chem. Commun. (1997) 2007.

21. (a) H. Arora, S.K. Barman, F. Lloret, R.N. Mukherjee, Inorg. Chem. 51 (2012) 5539; (b) K. Naik, A. Navrekar, D.G. Kokare, A. Kotian, V. Kamat, V.K. Revankar, J. Mol. Struct. 1125 (2016) 671.
22. O. Iranzo, A.Y. Kovalevsky, J.R. Morrow, J.P. Richard, J. Am. Chem. Soc. 125 (2003) 1988.
23. E. Kimura, T. Koike, Adv. Inorg. Chem. 44 (1997) 229.
24. J.E. Coleman, Curr. Opin. Chem. Biol. 2 (1998) 222.
25. B. Bauer-Siebenlist, F. Meyer, E. Farkas, D. Vidovic, S. Dechert, Chem. Eur. J. 11 (2005) 4349.
26. (a) C. Metcalfe, J.A. Thomas, Chem. Soc. Rev. 32 (2003) 215; (b) C.X. Zhang, S.J Lippard, Curr. Opin. Chem. Biol. 7 (2003) 481; (c) C. Liu, M. Wang, T. Zhang, H. Sun, Coord. Chem. Rev. 248 (2004) 147.
27. P. CA Bruijnincx, P.J Sadler, Curr. Opin. Chem. Biol. 12 (2008) 197.
28. A.M. Pizarro, P.J Sadler, Biochimie 91 (2009) 1198.
29. X. Sheng, X. Guo, X.-M. Lu, G.-Y. Lu, Y. Shao, F. Liu, Q. Xu, Bioconjugate Chem. 19 (2008) 490.
30. K. Ghosh, P. Kumar, N. Tyagi, U. P. Singh, Inorg. Chem. 49 (2010) 7614.
31. (a) M. Patel, M. Chhasatia, P. Parmar, Eur. J. Med. Chem. 45 (2010) 439; (b) Z. Kazemi, H.A. Rudbari, V. Mirkhani, M. Sahihi, M. Moghadam, S. Tangestaninejad, I. Mohammadpoor-Baltork, J. Mol. Struct. 1096 (2015) 110.
32. U.M. Rafi, D. Mahendiran, A.K.Haleel, R. P. Nankar, M. Doble, A.K. Rahiman, New J. Chem. 40 (2016) 2451.
33. SAINT PLUS, v.6.01, Bruker Analytical X-ray, Madison, WI, 1999.
34. SADABS v.2.01, Bruker/Siemens Area Detector Absorption Correction Program,Bruker AXS, Madison, Wisconsin, USA, 1998.
35. G.M. Sheldrick, Acta Crystallogr. A64 (2008) 112.
36. A.L. Spek, Acta Crystallogr. D65 (2009) 148.
37. C.F. Macrae, P. R. Edgington, P. McCabe, E. Pidcock, G. P. Shields, R. Taylor, M. Towler, J. Van de Streek, J. ApplCrystallogr. 39 (2006) 453.
38. A. Biswas, M.G.B. Drew, C. Diaz, A. Bauzá, A. Frontera, A. Ghosh, Dalton Trans.41 (2012) 12200.
39. R. Sanyal, A. Guha, T. Ghosh, T.K. Mondal, E. Zangrando, D. Das, Inorg. Chem. 53 (2014) 85.

40. M. Subat, K. Woinaroschy, S. Anthofer, B. Malterer, B. Konig, Inorg. Chem. 46 (2007) 4336.

41. A.B.P. Lever, Inorganic Electronic Spectroscopy, second ed., Elsevier, New York, 1984.

42. K. Nakamoto, Infrared and Raman Spectra of Inorganic and Coordination Compounds, Part B, fifth ed., John Wiley & Sons, New Jersey, 2009.

43. W. Addision, T. N. Rao, J. Reedijik, J. V. Rijn, G. C. Verschoor, J. Chem. Soc., Dalton Trans. (1984) 1349.

44. H.-Y. Chen, C.-C. Lin, Acta Crystallogr., E62 (2006) m1693.

45. A. Mukherjee, F. Lloret, R. Mukherjee, Inorg. Chem. 47 (2008)4471.

46. S. Bosch, P. Comba, L. R. Gaham, G. Schenk, Inorg. Chem,53 (2014) 9036.

47. R. Sanyal, X. Zhang, P. Kundu, T. Chattopadhyay, F. A. Mautner, D. Das, Inorg. Chem, 54 (2015) 2315.

48. Y.-L. Song, Y.-T. Li, Z.-Y. Wu, J. Inorg. Biochem. 101 (2007) 233.

Tables

Table 1. Crystallographic data for **1**-**3**

Crystal parameters CCDC No.	**1** 1522603	**2** 1522604	**3** 1522605
Formula Weight	$C_{24}H_{42}Cl_2N_4O_4Zn_2$ 652.30	$C_{22}H_{32}Br_2N_4O_2Zn_2$ 675.07	$C_{22}H_{34}I_2N_4O_2Zn_2$ 769.05
Crystal system	Orthorhombic	Triclinic	Triclinic
Space group	Aba2	P-1	P-1
a/Å	17.2388(9)	7.6106(8)	8.0004(7)
b/Å	17.4159(11)	13.0995(15)	13.0702(12)
c/Å	9.9579(5)	13.7770(15)	13.7450(13)
α/°	90	93.327(8)	91.570(4)
β/°	90	92.662(7)	94.751(4)
γ/°	90	105.768(7)	105.286(4)
V/Å^3	2989.7(3)	1316.8(3)	1379.8(2)
λ/Å	0.71073	0.71073	0.71073
σ_{calcd}/gm cm^{-3}	1.449	1.703	1.856
Z	4	2	2
T/K	296(2)	100(2)	100(2)
μ/mm^{-1}	1.818	4.881	4.000
F(000)	1360.0	676	752
ranges/°	4.702 to 28.411	1.484 to 24.878	4.342 to 27.996
h/k/l	-23,23/-23,23/-13,13	-8,8/-15,15/-16,16	-10,10/-17,17/-18,17
Reflections collected	38199	16991	24392
Independent reflections	3740	4418	6578
Data/restraints/parameters	3740/2/172	4418/0/291	6578/2/301
Goodness-of-fit on F^2	1.080	1.063	1.091
Final R indices [*I>2(I)*]	R1 = 0.0190 and wR2 = 0.0521	R1 = 0.0788 and wR2 = 0.1924	R1 = 0.0312 and wR2 = 0.0934
R indices (all data)	R1 = 0.0204 and wR2 = 0.0526	R1 = 0.1182 and wR2 = 0.2279	R1 = 0.0337 and wR2 = 0.0960
Largest peak and hole/eÅ^{-3}	0.221 and -0.287	1.627 and -1.730	1.676 and -1.219

Weighting scheme: $R = F_o\text{-}F_c/F_o$, $wR = [w(F_o^2\text{-}F_c^2)^2/w(F_o^2)^2]^{1/2}$

Table 2. Selected bond distances (Å) and bond angles (°) for **1**-**3**

1		**3**	
Zn1-O1a	2.0298(12)	Zn1-O1	2.0922(19)
Zn1-O1	2.0528(11)	Zn1-O2	1.993(2)
Zn1-N1	2.1835(18)	Zn1-N1	2.138(2)
Zn1-N2	2.162(2)	Zn1-N2	2.196(2)
Zn1-Cl1	2.2751(7)	Zn1-I1	2.5915(4)
O1-Zn1a	2.0298(12)	Zn2-O1	1.984(2)
O1a-Zn1-N2	139.70(9)	Zn2-O2	2.062(2)
O1-Zn1-N1	148.00(8)	Zn2-N3	2.164(3)
O1-Zn1-O1a	75.98(5)	Zn2-N4	2.196(3)
Zn1-O1-Zn1a	104.00(5)	Zn2-I2	2.6148(4)
N1-Zn1-N2	81.14(8)	O1-Zn1-O2	75.32(8)
O1-Zn1-N2	93.91(7)	O1-Zn1-N2	147.79(9)
O1a-Zn1-N1	87.45(7)	O2-Zn1-N1	142.46(9)
2		O1-Zn1-N1	85.82(8)
Zn1-O(2)	1.992(8)	O2-Zn1-N2	96.53(8)
Zn1-O(1)	2.082(7)	N1-Zn1-N2	82.36(9)
Zn1-N(1)	2.148(9)	O1-Zn2-O2	76.19(8)
Zn1-N(2)	2.182(8)	O1-Zn2-N3	141.15(9)
Zn1-BR2	2.4028(17)	O2-Zn2-N4	145.21(9)
Zn2-O(1)	1.987(8)	O1-Zn2-N4	93.97(9)
Zn2-O(2)	2.067(7)	O2-Zn2-N3	85.62(9)
Zn2-N(4)	2.139(10)	N3-Zn2-N4	81.69(10)
Zn2-N(3)	2.215(8)		
Zn2-BR4	2.4268(16)		
O(2)-Zn1-O(1)	75.0(3)		
O(2)-Zn1-N(1)	144.9(3)		
O(1)-Zn1-N(1)	85.9(3)		
O(2)-Zn1-N(2)	97.1(3)		
O(1)-Zn1-N(2)	147.2(3)		
N(1)-Zn1-N(2)	83.2(3)		
O(1)-Zn2-O(2)	75.4(3)		
O(1)-Zn2-N(4)	139.9(3)		
O(2)-Zn2-N(4)	86.2(3)		
O(1)-Zn2-N(3)	95.3(3)		
O(2)-Zn2-N(3)	147.2(3)		
N(4)-Zn2-N(3)	81.0(3)		

Symmetry code: a = -x, -y+1, z

Table 3. Hydrogen bonds donor/acceptor scheme (Å, °) for **1-3**

Compound	D-H···A	D-H	H···A	D···A	D-H···A	Symmetry codes
1	C(1)-H(13)...Cl(1)	0.97	2.83	3.788(3)	171	-x, 1/2-y, 1/2+z
	C(10)-H(11)...O(2)	0.97	2.55	3.496(5)	167	-1/2+x, 1-y, 1/2+z
	N(1)-H(111)...O(2)	0.86	2.55	3.228(4)	140.9	1/2-x,-1/2+y,z
	O(2)-H(112)...Cl(1)	0.82	2.52	3.234(3)	146	1/2+x,1-y,1/2+z
2	C(11)-H(11B)...Br(2)	0.99	2.89	3.641(13)	133	-1+x, y, z
3	N(1)-H(111)...I(1)	0.86	3.04	3.639(2)	129	-x,1-y,1-z
	C(2)-H(6)...I(1)	0.99	3.09	3.832(3)	132.4	-1+x, y, z

Table 4. Kinetic parameters calculated from Michaelis-Menten plot for **1-3**

Complex	$V_{max} \times 10^{-2}$ (M min^{-1})	$K_M \times 10^{-3}$(M)	K_{cat} (min^{-1})
1	2.95	5.5	590
2	1.67	3.44	334
3	3.52	6.36	705

Figures

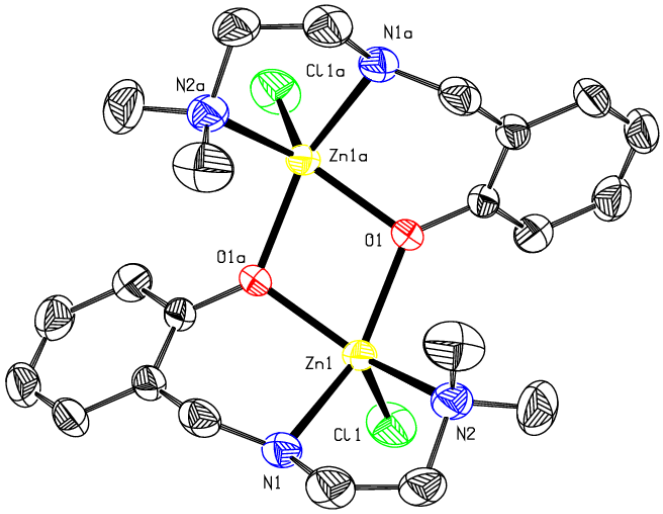

Fig. 1 An ORTEP diagram of the individual unit in **1** with the atom numbering scheme and 50% thermal ellipsoid probability (H atoms are omitted for clarity).

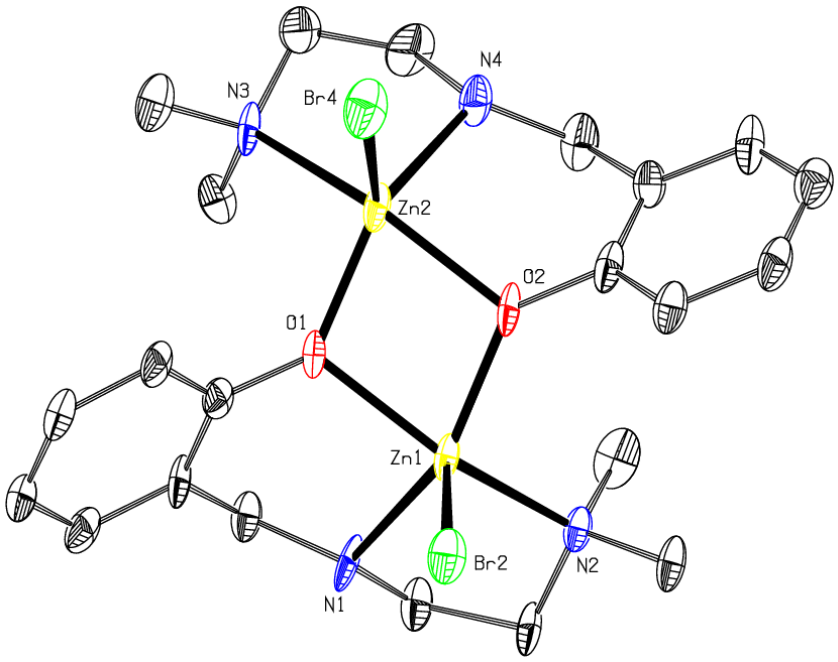

Fig. 2 Dinuclear unit in **2** (ORTEP; 50% probability ellipsoids). H atoms are omitted for clarity.

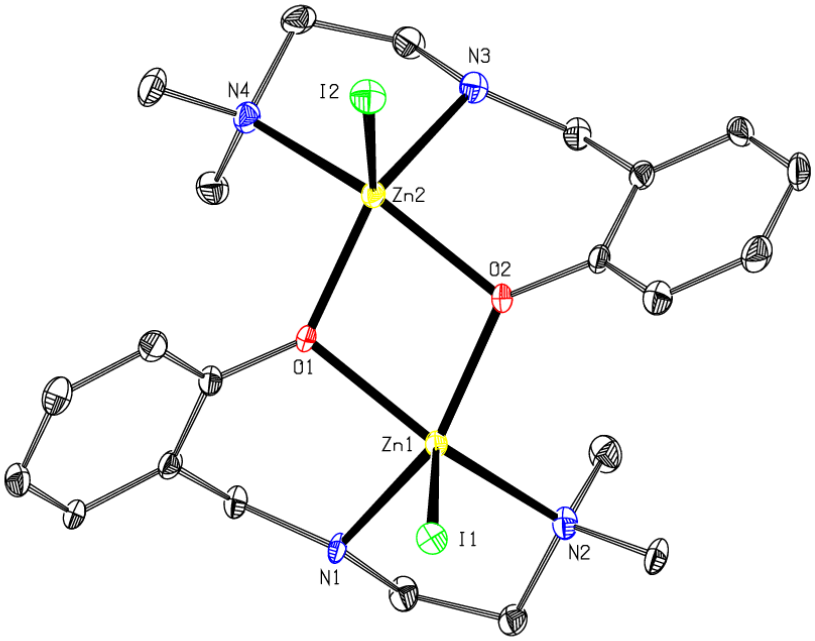

Fig. 3 Molecular structure of **3** (ORTEP; 50% probability ellipsoids). H atoms are omitted for clarity.

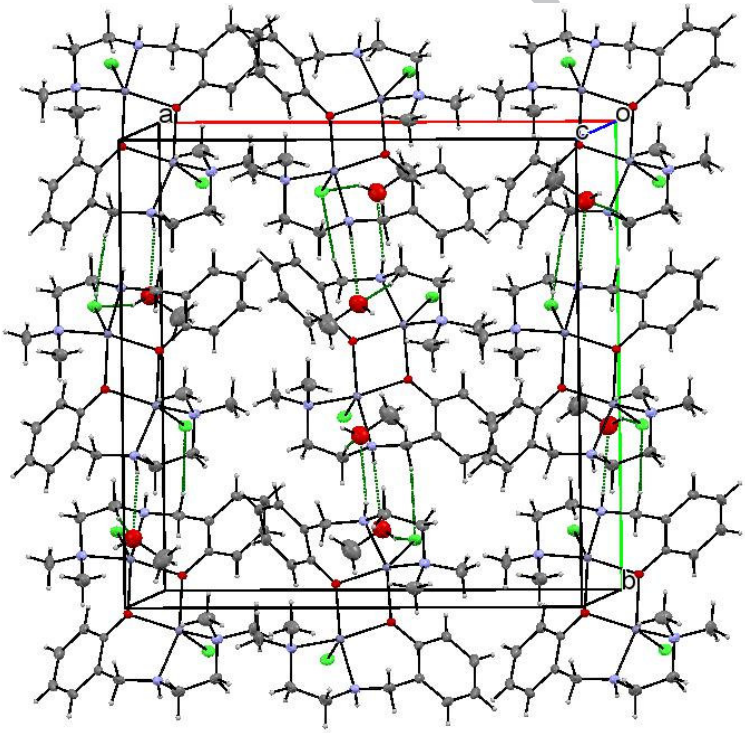

Fig. 4 Perspective view of the 2D sheet structure in **1** formed through inter-molecular hydrogen bonds along the *(100)*-plane.

(a)

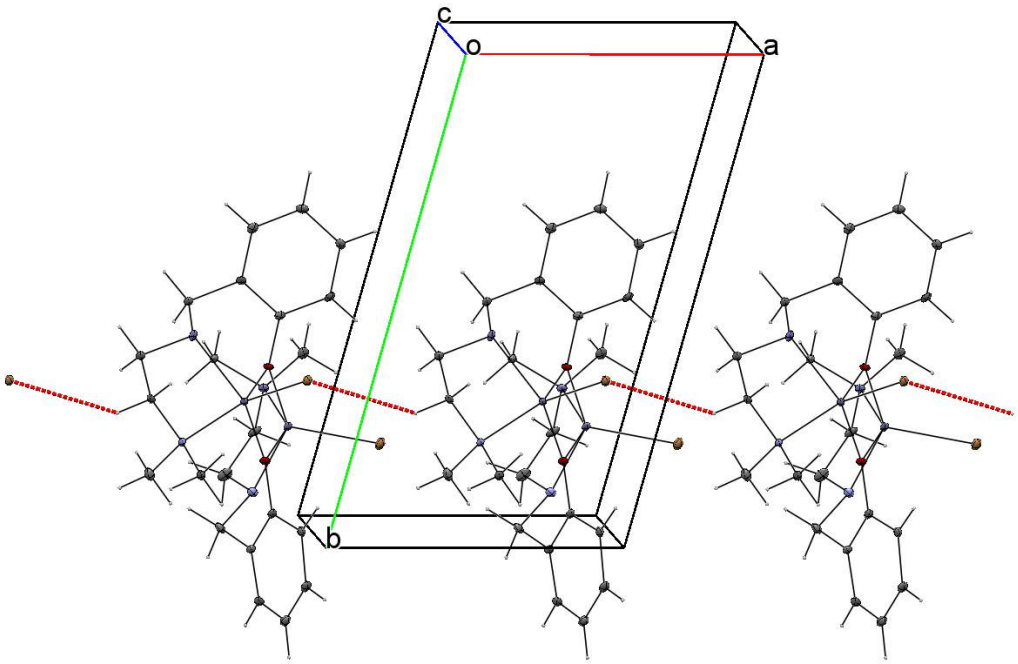

(b)

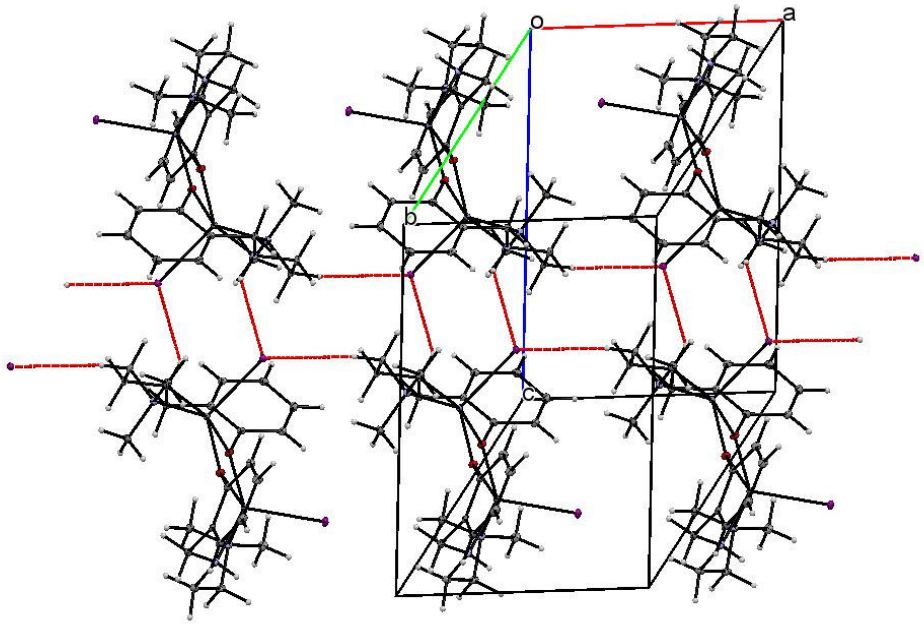

Fig. 5 Perspective view of different 1D chain structures (a) in **2** and (b) in **3** formed through inter-molecular C-H...X (X = Br in **2** and I in **3**) hydrogen bonds along the *a*-axis.

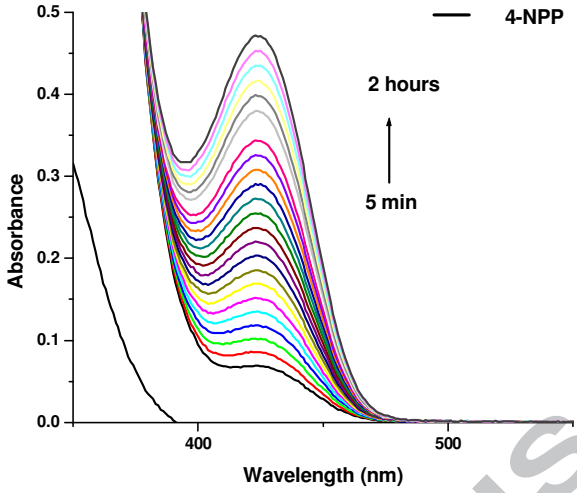

Fig. 6 Wavelength scan for the hydrolysis of 4-NPP in the absence and presence of **1** (substrate:catalyst = 20:1) in 97.5 % DMF at intervals of 5 minutes for 2 hours. [4-NPP] = 1 × 10^{-3} M, [Complex] = 0.05 × 10^{-3} M.

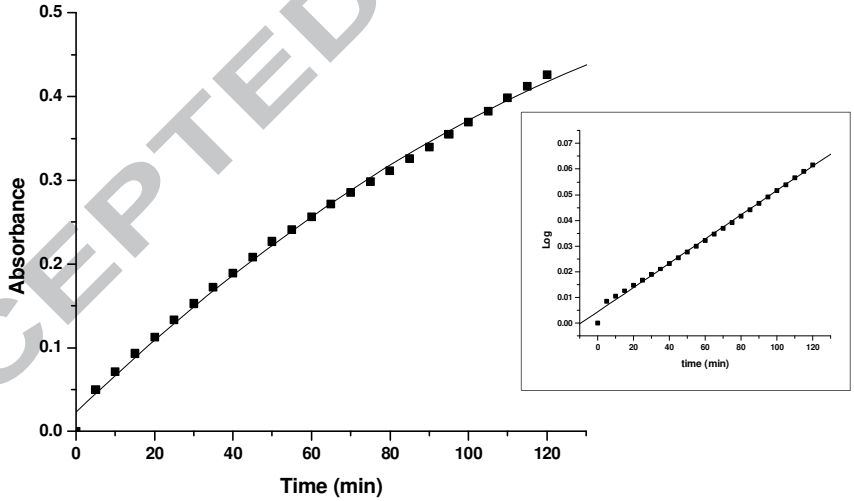

Fig. 7 Absorption vs time plot for complex **1** at 423 nm (least-squares fit of second order, R^2 = 0.997). Inset shows the plot of log[A_∞/(A_∞-A_t)] vs. time (R = 0.997).

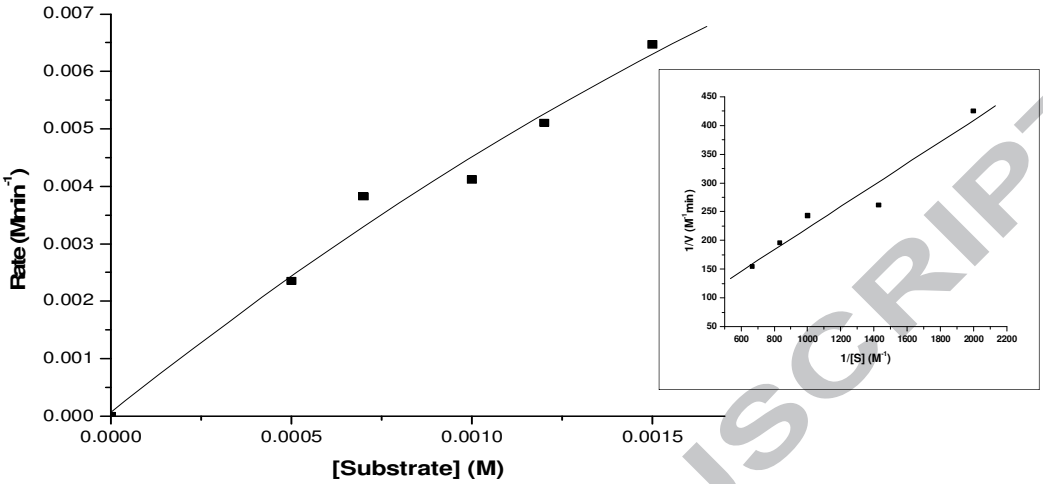

Fig. 8 Plot of enzymatic kinetics for **1** (Rate vs [Substrate], $R^2 = 0.980$). Inset shows the Lineweaver-Burk plot (1/V vs 1/[S]) having the intercept = 33.8677, slope = 0.18737 and R = 0.971.

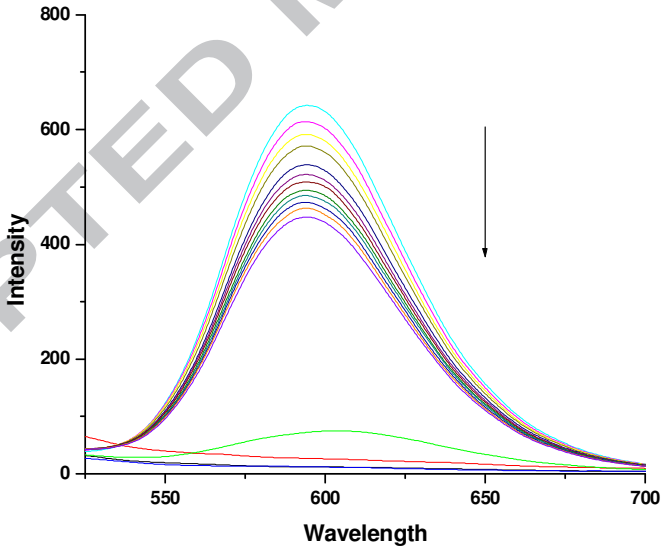

Fig. 9 Fluorescence emission profile associated with the binding of **1** with 37μM DNA at 298 K.

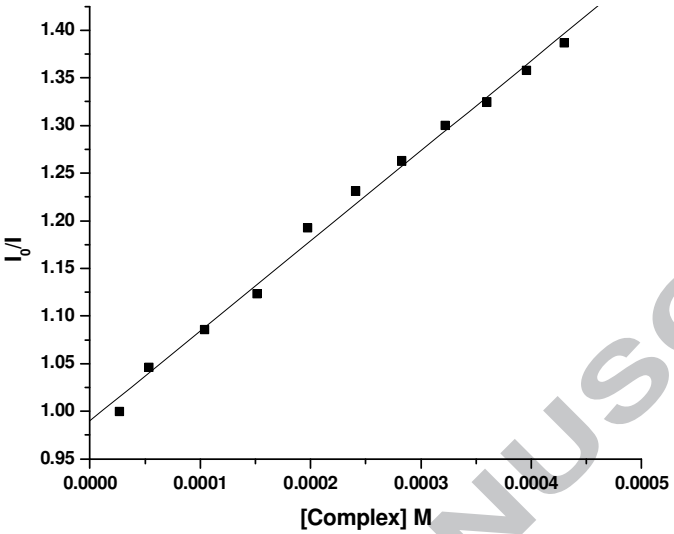

Fig. 10 Plot of I_o/I vs [complex] for the fluorescence quenching curves of EB bound to DNA by **1** (R = 0.995)

Phosphatase activity and DNA binding studies of dinuclear phenoxo-bridged zinc(II) complexes with an N,N,O-donor ligand and halide ions in a rare *cis*-configuration

Monika Sheoran[a], KishalayBhar[a], Tanveer A. Khan[a], Anuj K. Sharma[a] and Sunil G. Naik[a]*

Department of Chemistry, School of Chemical Sciences and Pharmacy, Central University of Rajasthan, NH-8, Bandarsindri, Ajmer Distt. Rajasthan, 305817

Graphical Abstract (Pictogram)

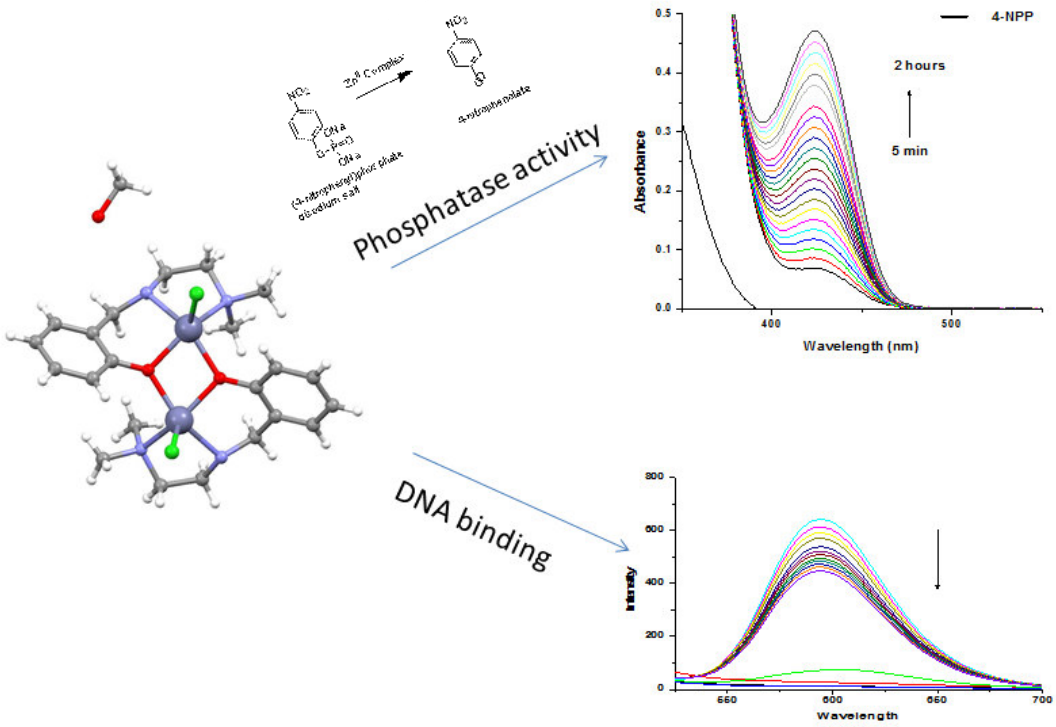

Phosphatase activity and DNA binding studies of dinuclear phenoxo-bridged zinc(II) complexes with an N,N,O-donor ligand and halide ions in a rare *cis*-configuration

Monika Sheoran[a], Kishalay Bhar[a], Tanveer A. Khan[a], Anuj K. Sharma[a] and Sunil G. Naik[a]*

Department of Chemistry, School of Chemical Sciences and Pharmacy, Central University of Rajasthan, NH-8, Bandarsindri, Ajmer Distt. Rajasthan, 305817

Graphical Abstract (Synopsis)

A tridentate NNO Schiff base ligand (HL) and its Zn(II) complexes of the types $[Zn_2(L)_2(Cl)]_2.2(CH_3OH)$ (**1**)and $[Zn_2(L)_2(X)]_2$ [X = Br (**2**), I (**3**)] have been synthesized and characterized by different spectroscopic techniques. The molecular structures of the three complexes were determined by single crystal X-ray crystallography. The initial rate values for the hydrolysis of 4-nitrophenylphosphate to 4-nitrophenolate by complexes **1**-**3** are respectively 590, 334 and 705 min^{-1}. The complexes show a weak external binding propensity to calf thymus DNA with binding constant values 9.45×10^2, 7.06×10^2, 6.51×10^2 M^{-1} for **1**, **2** and **3** respectively.

Reviewer #4: The authors have made significant corrections and improvements to the overall manuscript, however there are still some corrections to be made in terms of the crystallography of this paper.

I would recommend this paper for publication once the following corrections and considerations have been made.

Have the authors check for missed symmetry on PLATON for structures 2 and 3?

Reply: Yes, we have checked for missed symmetry on PLATON for structures 2 and 3. It shows 'no obvious change in symmetry needed'.

1. The chemical formula for 1 in the cif, contains an incomplete CH3OH moiety. Please can the authors correct this and the overall chemical formula.

Reply: Now we have corrected the formula of complex 1 by adding H-atoms to CH3OH moiety and NH- groups of ligands.

2. On page 3 line 58, while the H atoms have not been found (on all the NH groups), they need to still be included in the overall structure (where possible) and its formulas using the riding models (or fixed models if necessary). Corrections to this will need to be updated in the final CIF files.

Reply: Now for complexes 1 and 3 we have added the H-atoms to NH- groups of ligand and refined accordingly. But for complex 2 we are unable to locate such H-atoms. The corrected cifs are also submitted to CCDC.

3. The authors would also do well to note that the relatively low quality of data possibly due to the high-temperature of data collection does not provide a solid basis for detailed discussions of structural details and interactions.

Reply: According to honourable reviewer's suggestion we have modified the following structural part.

For example P8 line 37, 'In 1-3, Zn (II) centres show considerable deviations…' at this level of structural solutions and refinements, the comparisons and deviations are not necessarily considerable mainly due to the significant variation in the quality of the structure solution and refinement details.

It would be best to simply note the range of deviation if absolutely necessary.

Reply: According to honourable reviewer's suggestion we have omitted "P8 line 37, 'In 1-3, Zn (II) centres show considerable deviations" this description from structural details.

4. Similarly the deviation in the Zn-O distances, as discussed on P8, Line 54, 'more unsymmetrical' - should be 'more asymmetrical' or 'less symmetrical', although in 1, this is symmetrical.

Reply: According to honourable reviewer's suggestion we have also modified the discussed on deviation in the Zn-O distances in P8, Line 54, as 'less symmetrical, although in 1, this is symmetrical'.

5. Could the authors also consider the following in their discussion of the 'relationship between structure and catalytic activity'.

Reply: According to honourable reviewer's suggestion we have also modified this section as "The catalytic activity order of complexes **3>1>2** shows direct correspondence to the Zn...Zn separation (3.217 Å for **1**, 3.220 Å for **2** and 3.209 Å for **3**) indicating shorter Zn...Zn distance is better suited to accommodate the phosphate group."